

# High-throughput *ab initio* analysis of the Bi-In, Bi-Mg, Bi-Sb, In-Mg, In-Sb, and Mg-Sb systems

Stefano Curtarolo<sup>1,2</sup>, Aleksey N. Kolmogorov<sup>1</sup>, Franklin Hadley Cocks<sup>1</sup>

<sup>1</sup>*Department of Mechanical Engineering and Materials Science, Duke University, Durham, NC 27708*

<sup>2</sup>*corresponding author, e-mail: stefano@duke.edu*

(October 22, 2018)

Prediction and characterization of crystal structures of alloys are a key problem in materials research. Using high-throughput *ab initio* calculations we explore the low-temperature phase diagrams for the following systems: Bi-In, Bi-Mg, Bi-Sb, In-Mg, In-Sb, and Mg-Sb. For the experimentally observed phases in these systems we provide information about their stability at low temperatures. Keywords: Binary Alloys, *Ab initio*, Intermetallics, Transition Metals, Structure Prediction, Phase Stability, Magnesium, Indium, Bismuth, Antimony.

## I. INTRODUCTION

Magnesium alloys present an excellent combination of light weight and specific strength compared to steel and aluminum alloys and would offer an opportunity for radical improvement in automotive vehicle design and performance [1,2]. However, for more than fifty years magnesium alloy research has been confined almost exclusively to casting alloys and there has been no equivalent effort in developing wrought magnesium alloys of sufficiently high strength [3]. Both wrought aluminum alloys and wrought magnesium alloys achieve their increased strength levels through the process of precipitation-hardening, also known as age-hardening. In the case of aluminum alloys, the metallurgy of precipitation-hardening has been thoroughly explored and has resulted in the five and six element aluminum alloys which form the basis for all aerospace structures [4]. The trial and error research has required an enormous effort over many years to produce the aluminum alloys now in use. This is so because the hardening process depends on the development of stable and metastable phases in the base alloy matrix, a problem particularly difficult for experimental investigation due to long annealing times involved in the phase formation. If the development of greatly increased strength in precipitation-hardenable magnesium alloys followed a similar trial and error path it would require a similar level of effort [5].

Fortunately, the combination of *ab initio* density functional theory methods and data mining techniques provides an opportunity to dramatically accelerate materials research by efficiently predicting new phases and accurately describing their ground states [6–10]. These theoretical methods are particularly suitable for investigation of low-temperature compounds and can thus play an important role in the development of precipitation-hardenable magnesium alloys.

In this paper we systematically explore the low-temperature phase diagrams for the following six binary alloy systems: Bi-In, Bi-Mg, Bi-Sb, In-Mg, In-Sb, and Mg-Sb. Both Mg-Bi and Mg-Sb systems have the poten-

tial to be new age-hardenable magnesium-based alloys. Indium is of interest because it is one of the very few elements with high solubility in magnesium and yet has low electrochemical activity; whereby the relatively high electrochemical activity of magnesium might reasonably be expected to be reduced, albeit at an increase in overall alloy density. The In-Sb and In-Bi systems are included to complete the possibilities for binary alloys among these elements.

The Binary Alloy Phase Diagrams [11] and the Pauling File [12] give a broad review of experimental data on these systems. In most cases the experimental results are complemented by thermodynamic modeling [11–13]. However, to the best of our knowledge, *ab initio* studies regarding phase stabilities in these systems are scarce [14–16]. To check the completeness of the experimentally known phase diagrams in these systems and provide information on the phase stabilities at low temperatures we have chosen a large library of most common prototypes in binary alloys and calculated ground state energies of these structures with *ab initio* methods.

We describe the prototype library in the next section, give the details of the *ab initio* methods used in this study in section “High-throughput First Principles calculations”, and present the results for each of the six systems in section “Alloys”.

## II. BINARY SYSTEMS AND STRUCTURE PROTOTYPES

We calculate six alloys, Bi-In, Bi-Mg, Bi-Sb, In-Mg, In-Sb, and Mg-Sb in 186 crystal structure configurations. Many of these configurations have the same prototype, for example,  $AB_3$  and  $A_3B$  so the number of distinct prototypes is 108. The various concentrations are listed in the following table.

Compounds composition	Conc. of B	number of prototypes
A & B	0%	6
A <sub>5</sub> B & AB <sub>5</sub>	16.66%	3
A <sub>4</sub> B & AB <sub>4</sub>	20%	2
A <sub>3</sub> B & AB <sub>3</sub>	25%	27
A <sub>2</sub> B <sub>5</sub> & A <sub>5</sub> B <sub>2</sub>	28.57%	1
A <sub>2</sub> B & AB <sub>2</sub>	33.33%	34
A <sub>5</sub> B <sub>3</sub> & A <sub>3</sub> B <sub>5</sub>	37.5%	3
A <sub>3</sub> B <sub>2</sub> & A <sub>2</sub> B <sub>3</sub>	40%	2
A <sub>4</sub> B <sub>3</sub> & A <sub>3</sub> B <sub>4</sub>	42.85%	1
AB (& BA*)	50%	29 (+3)

TABLE 1. Compositions, concentrations and number of prototypes in the library. The library has 186 structures, and 108 distinct prototypes (\* at composition AB, 3 prototypes have different point groups in atomic positions A and B, therefore they represent distinct structure types).

Of such prototypes, 67 are chosen from the most common intermetallic binary structures in the Pauling File [12] and the CRYSTMET database [13], plus the common low temperature compounds (5) reported for the Mg, In, Sb and Bi systems [11,12]. Such prototypes can be described by their Strukturbericht designation and/or natural prototypes [11,12]: A1, A2, A3, A4, A6, A7, A15, B<sub>h</sub>, B1, B2, B3, B4, B8<sub>1</sub>, B8<sub>2</sub>, B10, B11, B19, B27, B32, B33 (B<sub>f</sub>), C<sub>c</sub>, C2, C6, C11<sub>b</sub>, C14, C15, C15<sub>b</sub>, C16, C18, C22, C32, C33, C37, C38, C49, D0<sub>a</sub>, D0<sub>3</sub>, D0<sub>9</sub>, D0<sub>11</sub>, D0<sub>19</sub>, D0<sub>22</sub>, D0<sub>23</sub>, D0<sub>24</sub>, D1<sub>3</sub>, D1<sub>a</sub>, D2<sub>d</sub>, D5<sub>2</sub>, D7<sub>3</sub>, D8<sub>8</sub>, D8<sub>g</sub>, L1<sub>0</sub>, L1<sub>1</sub>, L1<sub>2</sub>, L6<sub>0</sub>, CaIn<sub>2</sub>, Cr<sub>3</sub>B<sub>5</sub>, CuTe, CuZr<sub>2</sub>, GdSi<sub>2</sub> (1.4), Mg<sub>2</sub>In, MoPt<sub>2</sub>, NbAs (NbP), NbPd<sub>3</sub>, Ni<sub>2</sub>In, Ni<sub>2</sub>Si, Ω (with z=1/4), Pu<sub>3</sub>Al (Co<sub>3</sub>V), Ti<sub>3</sub>Cu<sub>4</sub>, W<sub>5</sub>Si<sub>3</sub>, YCd<sub>3</sub>, ZrSi<sub>2</sub>, γ-Ir. The rest of the structures (36) are fcc, bcc or hcp superstructures. Twelve of these superstructures consist of stacking of pure A and B planes along some common direction [6,17].

### III. HIGH-THROUGHPUT FIRST PRINCIPLES CALCULATIONS

The high-throughput *ab initio* method used for this project is fully described in references [6,7]. A summary of the details of the calculations is given below.

**Ultra Soft Pseudopotentials LDA calculations (US-LDA).** The energy calculations were performed using Density Functional Theory in the Local Density Approximation (LDA), with the Ceperley-Alder form for the correlation energy as parameterized by Perdew-Zunger [18] and with ultra soft Vanderbilt type pseudopotentials [19], as implemented in VASP [20]. Calculations are done at zero temperature and pressure, with spin polarization, and without zero-point motion. The energy cutoff in an alloy was set to 1.5 times the larger of the suggested energy cutoffs of the pseudopotentials of the elements of the alloy (suggested energy cutoffs are derived by the method described in [20]). Brillouin zone integrations

were performed using at least 3500/(number of atoms in unit cell) **k**-points distributed on a Monkhorst-Pack mesh [21,22]. With these energy cutoffs and **k**-points meshes the absolute energy is converged to better than 10 meV/atom. Energy differences between structures are expected to be converged to much smaller tolerances. All structures were fully relaxed.

**PAW-GGA calculations.** When several structures are in close competition for the ground state, we also performed calculations in the Generalized Gradient Approximation (GGA), with Projector Augmented-Wave (PAW) pseudopotentials, as implemented in VASP [20,23,24]. In general, we expect the PAW-GGA approach to be more accurate than the US-LDA. For the GGA correlation energy, we used the Perdew-Wang parameterization (GGA-PW91) [25]. Compared to the US-LDA case, we use an increased energy cutoff of 1.75 times the larger of the suggested energy cutoffs for the elements in the system and a finer **k**-point mesh with at least ~4000/(number of atoms in unit cell).

**Symmetries of the pure elements.** Our calculations reproduce the correct experimental crystal structures of the pure elements at room temperature. Bi and Sb are most stable in the A7 structure ( $\alpha$ -As prototype), while Mg and In have hexagonal closed packed (A3) and face-centered tetragonal (A6) structures, respectively.

**Calculation of the formation energies and the convex hull.** The formation energy for each structure is determined with respect to the most stable structure of the pure elements. To determine the ground states of a system one needs to find, as a function of composition, the ordered compounds that have an energy lower than any other structure or any linear combination of structures that gives the proper composition. This set of ground state structures forms a *convex hull*, as all other structures have an energy that falls above the set of tie lines that connects the energy of the ground states. In thermodynamical terms, the *convex hull* represents the Gibbs free energy of the alloy at zero temperature.

## IV. ALLOYS

### Bi-In (Bismuth - Indium)

The phase diagram of the Bi-In system is known from experimental investigations and thermodynamic modeling [11,12,26–32]. Three phases are expected to be stable at low temperatures: BiIn-B10, BiIn<sub>2</sub>-InNi<sub>2</sub>, and Bi<sub>3</sub>In<sub>5</sub>-Cr<sub>3</sub>B<sub>5</sub>. However, the evidence for the low-temperature stability of BiIn<sub>2</sub> and Bi<sub>3</sub>In<sub>5</sub> is not conclusive [27]. With our US-LDA calculations, we have found that only three phases have negative formation energy. These phases BiIn-B10, BiIn<sub>2</sub>-InNi<sub>2</sub>, and a monoclinic structure with space group C2/m #12 at 50% concentration have formation energies equal to -17 meV/atom, -4.4 meV/atom, and -7.9 meV/atom, respectively. Therefore, phase diagram calculated in US-LDA has only one stable compound, BiIn-B10; the other two experimentally observed stable phases BiIn<sub>2</sub> and Bi<sub>3</sub>In<sub>5</sub> are above the convex hull by 6.3 and 26 meV/atom, respectively.

Bi-In system		
Low Temperature Phases comparison chart		
Composition % Bi	Experimental (Massalski [11])	<i>Ab initio</i> result
33.3	BiIn <sub>2</sub> -InNi <sub>2</sub>	two phase region (us-lda) BiIn <sub>2</sub> -InNi <sub>2</sub> is ~6.3 meV/at. higher than the tie-line In ↔ BiIn <i>BiIn<sub>2</sub> stable (paw-gga)</i>
37.5	Bi <sub>3</sub> In <sub>5</sub> -Cr <sub>3</sub> B <sub>5</sub>	Bi <sub>3</sub> In <sub>5</sub> unstable us-lda and <i>paw-gga</i>
50	BiIn-B10	BiIn-B10 $E_f = -17$ meV/at. (us-lda) $E_f = -6$ meV/at. ( <i>paw-gga</i> )

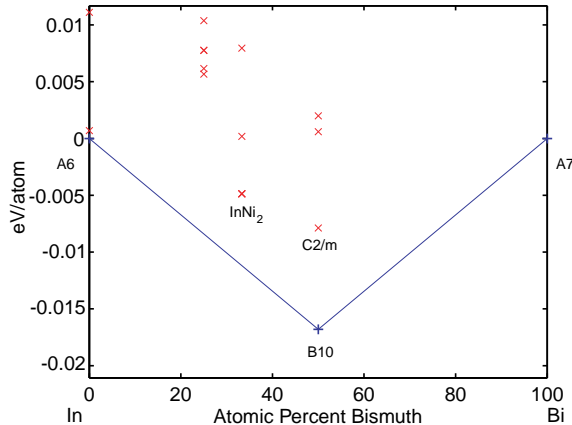


FIG. 1. Bi-In (Bismuth - Indium) ground state convex hull calculated in US-LDA.

Due to the rather small energy differences and overall low formation energies we further investigate the phase diagram with the PAW-GGA potentials, as described in the method section. With PAW-GGA, we find that BiIn-B10 has less negative formation energy, -6 meV/atom, and therefore BiIn<sub>2</sub>-InNi<sub>2</sub> becomes stable by having its energy 3.1 meV/atom below the tie-line In ↔ BiIn. The

monoclinic structure with space group C2/m #12 at 50% concentration is now unstable having the formation energy of 10 meV/atom. The Bi<sub>3</sub>In<sub>5</sub> phase still has positive formation energy (22 meV/atom) and remains significantly higher the tie-line InNi<sub>2</sub> ↔ InBi (by 29 meV/atom). In summary, our results suggest that at low temperatures BiIn<sub>2</sub> may be stable, while Bi<sub>3</sub>In<sub>5</sub> is likely to be unstable.

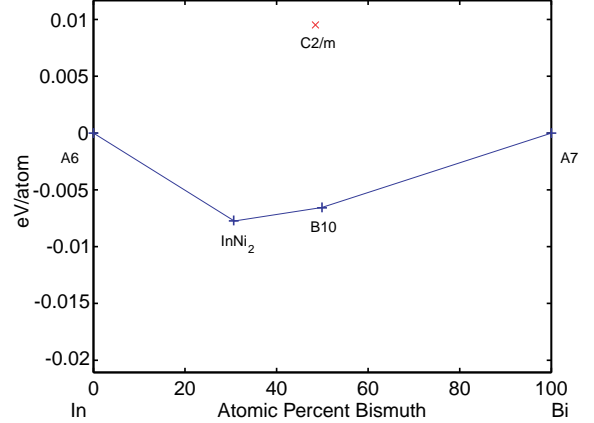


FIG. 2. Bi-In (Bismuth - Indium) ground state convex hull calculated in PAW-GGA.

### Bi-Mg (Bismuth - Magnesium)

Only one stable compound has been observed for the Mg-Sb system at low temperatures:  $\alpha$ Bi<sub>3</sub>Mg<sub>2</sub>-La<sub>3</sub>O<sub>2</sub> [11,12,33–35]. Our calculations confirm the low-temperature stability of this phase with a formation energy of -252 meV/atom. We have not found any other stable compounds for this system, therefore the experimental low temperature part of the diagram is complete.

Bi-Mg system		
Low Temperature Phases comparison chart		
Composition % Bi	Experimental (Massalski [11])	<i>Ab initio</i> result
40	D5 <sub>2</sub>	Bi <sub>3</sub> Mg <sub>2</sub> -D5 <sub>2</sub> (us-lda) $E_f = -252$ meV/at.

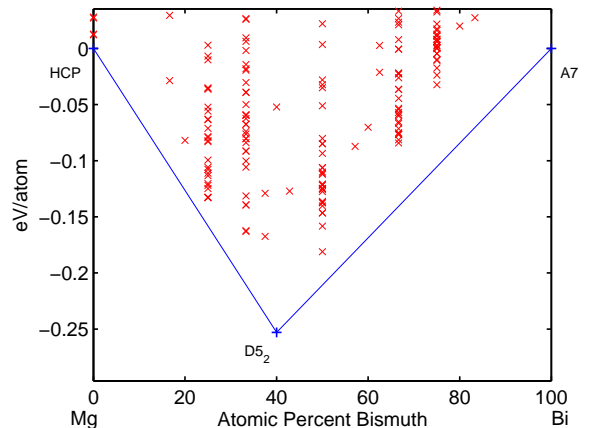


FIG. 3. Bi-Mg (Bismuth - Magnesium) ground state convex hull.

### Bi-Sb (Bismuth - Antimony)

No intermediate stable compounds have been reported for the Bi-Sb system and it is considered to be a non-compound forming system [11,12]. Our calculations confirm the absence of any stable phases. The structure with lowest formation energy in the whole range of concentrations is found to be BiSb-B1 with  $E_f=21$  meV/atom.

### In-Mg (Indium - Magnesium)

Five ordered compounds have been reported for the system Mg-In at low temperatures [11,12,36–41]:  $Mg_{1.2}In_{2.8}-L1_2$  ( $\gamma'$ ),  $MgIn-L1_0$  ( $\beta''$ ),  $Mg_2In$  (prototype,  $\beta_2$ ,  $Mg_2Tl$  in [11]),  $Mg_5In_2-D8_g$  ( $\beta_3$ ), and  $Mg_3In$  ( $\beta_1$ ) with Pearson symbol hR48, and space group R $\bar{3}m$  (#166) [11,12] (note that  $\beta_1$  has Pearson symbol hR16 in Massalski [11]). At high temperatures phase  $\beta_1$  transforms into the  $L1_2$  structure, which is similar to the high temperature field  $\beta'$ . Phases  $\beta_1$  and  $\beta'$  share a eutectoid reaction at 202°C ( $\beta' \leftrightarrow \beta_1 + \beta_3$  at  $\sim 27.5\%$  of In), and a peritectoid reaction at 337°C ( $\beta_1 \leftrightarrow \beta + \beta'$  at  $\sim 24\%$  of In). Therefore we expect the morphology of  $\beta_1$  to be similar to  $L1_2$  (with partial occupation) and to find the structure  $Mg_3In-L1_2$  under the tie-line  $In-A6 \leftrightarrow MgIn-L1_0$  at zero temperature.

In-Mg system		
Low Temperature Phases comparison chart		
Composition % In	Experimental (Massalski [11])	<i>Ab initio</i> result
$\sim 26$ to $38.5$	$Mg_3In$ ( $\beta_1$ ) hR48 R $\bar{3}m$ [12] (low T), $\sim L1_2$ (high T)	$L1_2$
28.6	$Mg_5In_2-D8_g$ ( $\beta_3$ )	two phase region $D8_g$ is 4.9 meV/at. above $\beta_1 \leftrightarrow \beta_2$ (us-lda) $D8_g$ is 5.4 meV/at. above $\beta_1 \leftrightarrow \beta_2$ (paw-gga)
$\sim 34$	$Mg_2In$ ( $\beta_2$ )	$Mg_2In$ stable $\sim 3.5$ meV/at. below $L1_2 \leftrightarrow L1_0$ (us-lda) $\sim 1$ meV/at. below $L1_2 \leftrightarrow L1_0$ (paw-gga)
$\sim 39$ to $59$	$MgIn-L1_0$ ( $\beta''$ )	$L1_0$
$\sim 69.5$ to $75.5$	$Mg_{1.2}In_{2.8}-L1_2$ ( $\gamma'$ )	$MgIn_3-L1_2$

The off-stoichiometry  $Mg_{1.2}In_{2.8}-L1_2$  phase is not subject of our investigation, since it requires simulations of disordered systems. With our calculations, we find the ordered phase  $MgIn_3-L1_2$  to be stable. Two competing Long Period Superstructures of  $MgIn_3-L1_2$ ,  $D0_{23}$  and  $D0_{24}$ , are less favorable than the  $L1_2$  phase by  $\sim 2.5$  and  $\sim 5.7$  meV/atom, respectively. This suggests that long-range interactions are weak in this system at composition  $MgIn_3$ . We confirm the stability of  $MgIn-L1_0$  ( $\beta''$ ),  $Mg_2In-\beta_2$ , and  $MgIn_3-L1_2$  phases but find that  $Mg_5In_2-D8_g$  lies 4.9 meV/atom above the tie-line  $Mg_3In-\beta_1 \leftrightarrow Mg_2In-\beta_2$ . Besides,  $Mg_2In-\beta_2$  is stable but with a relative stability energy of 3.5 meV/atom below the tie-line  $Mg_3In \leftrightarrow MgIn$ , which is within the error of present

calculations. We find a metastable compound,  $MgIn_2-C_c$ , to be  $\sim 2.7$  meV/atom above the tie-line  $MgIn \leftrightarrow MgIn_3$ . This compound might become stable at higher temperatures and pressures. We recalculate the phase diagram with PAW-GGA potentials and find essentially no difference compared to the US-LDA results:  $Mg_2In-\beta_2$  is 1 meV/atom below the  $Mg_3In \leftrightarrow MgIn$  tie-line,  $Mg_5In_2-D8_g$  is above the  $Mg_3In-\beta_1 \leftrightarrow Mg_2In-\beta_2$  by 5.4 meV/atom and  $MgIn_2-C_c$  remains metastable by 4.6 meV/atom. In summary, our calculations confirm the low temperature part of the Mg-In diagram known from experiment. The results show that  $Mg_5In_2-D8_g$  may not be stable at low temperatures. In addition, we identify a metastable phase,  $MgIn_2-C_c$ , which might be stable at higher pressures and temperatures.

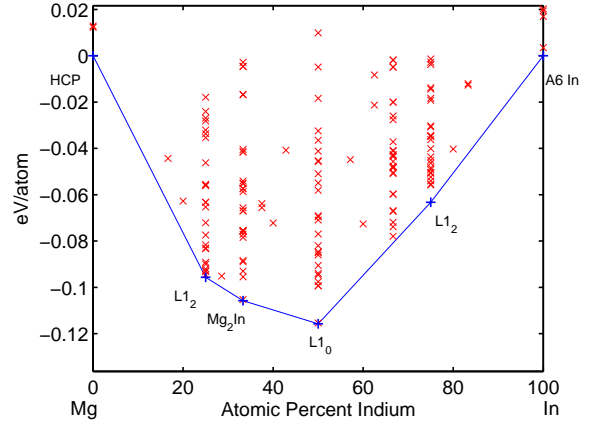


FIG. 4. In-Mg (Indium - Magnesium) ground state convex hull.

## In-Sb (Indium - Antimony)

The phase diagram of the system In-Sb is based on a single compound  $\alpha$ InSb-B3 [11,12,42–47]. It is well studied at high pressures and temperatures where other modifications of InSb ( $\beta$ InSb,  $\gamma$ InSb, and  $\delta$ InSb) have been observed [28,45]. The high-pressure transitions have also been thoroughly studied with *ab initio* methods [15,16]. At zero pressure our calculations confirm the experimental stability of the low temperature compound  $\alpha$ InSb-B3. The InSb-B10 phase, stable for the similar binary system In-Bi at 50% concentration, here is unstable with an energy  $\sim 105$  meV/atom higher than  $\alpha$ InSb-B3. We do not observe any other stable compounds for the In-Sb system and conclude that the low temperature experimental characterization of the system is complete.

In-Sb system		
Low Temperature Phases comparison chart		
Composition % Sb	Experimental (Massalski [11])	<i>Ab initio</i> result
50	B3	$\alpha$ InSb-B3 B10 $\sim 105$ meV/at. higher than B3 (us-lda)

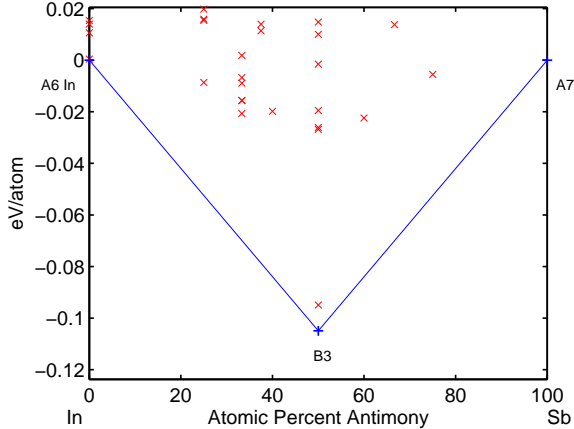


FIG. 5. In-Sb (Indium - Antimony) ground state convex hull.

## Mg-Sb (Magnesium - Antimony)

Similarly to the Bi-Mg system the Mg-Sb system has only one stable compound at low temperature:  $\alpha$ Mg<sub>3</sub>Sb<sub>2</sub>-B5<sub>2</sub> [12,11,48,35,49–51]. Interestingly, there is no solid solubility for Mg in Sb or Sb in Mg, although Mg and Sb have similar dimensions (atomic radius ratio Sb/Mg=1.09) [11]. At high temperatures phase  $\alpha$ Mg<sub>3</sub>Sb<sub>2</sub>-B5<sub>2</sub> undergoes a polymorphic change, as reported in [35]. To our knowledge, there is no information about the stability of  $\alpha$ Mg<sub>3</sub>Sb<sub>2</sub>-B5<sub>2</sub> below 450°C and it is unclear how far this stable phase extends into the low temperature region. Our calculations confirm that this compound remains stable at low temperatures having the formation energy of -404 meV/atom. No other

stable compounds have been found for this system, therefore the experimentally known low-temperature part of the phase diagram is complete.

Mg-In system		
Low Temperature Phases comparison chart		
Composition % Sb	Experimental (Massalski [11])	<i>Ab initio</i> result
40	D5 <sub>2</sub>	Mg <sub>3</sub> Sb <sub>2</sub> -D5 <sub>2</sub>

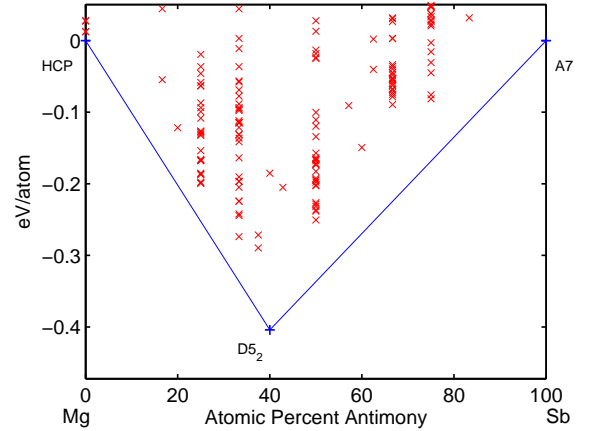


FIG. 6. Mg-Sb (Magnesium - Antimony) ground state convex hull.

## V. CONCLUSIONS

The results of our systematic *ab initio* study of the six binary systems Bi-In, Bi-Mg, Bi-Sb, In-Mg, In-Sb, and Mg-Sb suggest that the experimentally known low-temperature phase diagrams for these alloys are complete. Using the calculated ground state energies we complement experimental information on the stability of several phases in the limit of low temperature and zero pressure: phase  $\alpha$ Mg<sub>3</sub>Sb<sub>2</sub>-B5<sub>2</sub> is stable, phase Mg<sub>5</sub>In<sub>2</sub>-D8<sub>g</sub> may not be stable and phase Bi<sub>3</sub>In<sub>5</sub> is likely to be unstable. We find that compound MgIn<sub>2</sub>-C<sub>c</sub>, not observed experimentally, is metastable but very close to stability and could therefore exist at different temperatures and pressures. Further theoretical investigation of these structures and search for other (meta)stable phases at finite temperatures and pressures should include thermodynamic effects.

## VI. ACKNOWLEDGMENTS

This research has benefited from discussion with Gerbrand Ceder, Dane Morgan, Milton Cole, Renee Diehl and Zi-Kui Liu.

- 
- [1] A. A. Luo, *J. of Metals* **54** (2), 42-48 (2002).
- [2] B. R. Powell, *J. of Metals* **55** (11), 28-29 (2003).
- [3] D. Eliezer, E. Aghion, and F. H. Froes, *Advanced Performance Materials* **5**, 201-212 (1998).
- [4] *Metals Handbook*, 10th edition, Vol. 2, *Properties and Selection: Nonferrous Alloys and Special-Purpose Materials*, The American Society for Metals, pp. 62-122 (1990).
- [5] *Precipitation Processes in Solids*, edited by K. C. Russell and H. I. Aaronson, The Metallurgical Society of AIME, pp. 87-120 (1978).
- [6] S. Curtarolo, D. Morgan, K. Persson, J. Rodgers, and G. Ceder, *Phys. Rev. Lett.* **91**, 135503 (2003).
- [7] S. Curtarolo, D. Morgan, and G. Ceder, *Calphad*, in press (2005).
- [8] D. Morgan, G. Ceder, and S. Curtarolo, *Mat. Res. Soc. Symp. Proc.* **804**, JJ9.25 (2004).
- [9] D. Morgan, G. Ceder, and S. Curtarolo, *Meas. Sci. Technol.* **16** 296-301 (2005).
- [10] Y. Wang, S. Curtarolo, C. Jiang, R. Arroyave, T. Wang, G. Ceder, L.-Q. Chen, and Z.-K. Liu, *Calphad* **28**, 79 (2004).
- [11] *Binary Alloy Phase Diagrams*, edited by T. B. Massalski (ASM International, Metals Park, OH, 1992)
- [12] P. Villars, K. Cenzual, J. L. C. Daams, F. Hulliger, T. B. Massalski, H. Okamoto, K. Otsaki, A. Prince, and S. Iwata, *Crystal Impact, Pauling File. Inorganic Materials Database and Design System*, Binaries Edition, ASM International, Metal Park, OH (2003)
- [13] P. S. White, J. R. Rodgers, and Y. Le Page, *CRYSTMET: a database of the structures and powder patterns of metals and intermetallics*, *Acta Cryst. B* **58**, 343 (2002).
- [14] G. A. de Wijs, G. Pastore, A. Selloni, W. van der Lugt, *J. Phys.: Cond. Matt.* **8**, 1879-1896 (1996).
- [15] G. Y. Guo, J. Crain, P. Blaha, W. M. Temmerman, *Phys. Rev. B* **47**, 4841-4848 (1993).
- [16] A. A. Kelsey and G. J. Ackland, *J. Phys. : Cond. Matt.* **12**, 7161-7173 (2000).
- [17] S. Curtarolo, *Coarse-Graining and Data Mining Approaches to the Prediction of Structures and their Dynamics*, Ph.D. Thesis, MIT (2003).  
Download: [burgaz.mit.edu](http://burgaz.mit.edu) and [alpha.mems.duke.edu](http://alpha.mems.duke.edu)
- [18] J. P. Perdew and A. Zunger, *Phys. Rev. B* **23**, 5048 (1981).
- [19] D. Vanderbilt, *Phys. Rev. B* **41**, 7892 (1990).
- [20] G. Kresse and J. Furthmuller, *Comput. Mater. Sci.* **6**, 15 (1996).
- [21] H. J. Monkhorst and J. D. Pack, *Phys. Rev. B* **13**, 5188 (1976).
- [22] J. D. Pack and H. J. Monkhorst, *Phys. Rev. B* **16**, 1748 (1977).
- [23] P. E. Blöchl, *Phys. Rev. B* **50**, 17953 (1994).
- [24] G. Kresse and D. Joubert, *Phys. Rev. B* **59**, 1758 (1999).
- [25] J. P. Perdew and Y. Wang, *Phys. Rev. B* **45**, 13244 (1992).
- [26] B. C. Giessen, M. Morris, and N. J. Grant, *Trans. Metall. Soc. AIME* **239**, 883-889 (1967).
- [27] R. Boom, P. C. M. Vendel, and F. R. deBoer, *Acta Metall.* **21**, 807-812 (1973).
- [28] V. F. Degtyareva, S. A. Ivakhnenko, E. G. Ponyatovskii, and V. I. Rashchupkin, *Sov. Phys. Solid State* **24**, 770-774 (1982).
- [29] D. S. Evans and A. Prince, *Met. Sci.* **17**, 117-121 (1983).
- [30] P. Y. Chevalier, *Calphad* **12**, 383-392 (1988).
- [31] Y. Cui, S. Ishihara, X. J. Liu, I. Ohnuma, R. Kainuma, H. Ohtani, and K. Ishida, *Materials Transactions* **43**, 1879-1886 (2002).
- [32] S. Canegallo, V. Demeneopoulos, L. P. Bicelli, and G. Serravalle, *J. Alloys Compd.* **216**, 149-154 (1994).
- [33] M. Wobst, *Z. Phys. Chem.* **219**, 239-265 (1962).
- [34] C. S. Oh, S. Y. Kang, and D. N. Lee, *Calphad* **16**, 181-191 (1992).
- [35] G. Grube and R. Bornhak, *Z. Elektrochem.* **40**, 140-142 (1934).
- [36] W. Hume-Rothery and G. V. Raynor, *J. Inst. Met.* **63**, 201-216 (1938).
- [37] G. V. Raynor, *Trans. Faraday Soc.* **44**, 15-28 (1948).
- [38] K. Hiraga, M. Koiwa, and M. Hirabayashi, *J. Less-Common Met.* **15**, 109-119 (1968).
- [39] K. M. Pickwick, W. A. Alexander, and R. H. Gamble, *Can. J. Chem.* **47**, 3417-3427 (1969).
- [40] P. Feschotte, *J. Less-Common Met.* **46**, 51-54 (1976).
- [41] Y. Watanabe, *Acta Metall.* **23**, 691-696 (1975).
- [42] S. A. Pogodin and S. A. Dubinsky, *Izv. Sektora. Fiz. - Khim. Anal.* **17** 204-208 (1949), in Russian.
- [43] T. S. Liu and E. A. Peretti, *Trans. ASM* **44**, 539-548 (1952).
- [44] R. N. Hall, *J. Electrochem. Soc.* **110**, 385-388 (1963).
- [45] V. F. Degtyareva, T. Belash, G. V. Chipenko, E. G. Ponyatovskii, and V. I. Rashchupkin, *Sov. Phys. Solid State* **25**, 1712-1715 (1983).
- [46] V. I. Goryacheva, V. A. Geiderikh, and Y. I. Gerasimov, *Russ. J. Phys. Chem.* **57**, 1637-1639 (1983).
- [47] V. M. Kozlov, V. Agrigento, D. Bontempi, S. Canegallo, C. Moraitou, A. Toussimi, L. P. Bicelli, and G. Serravalle, *J. Alloys Compd.* **259**, 234-240 (1997).
- [48] G. Grube, *Z. Anorg. Chem.* **49**, 87-91 (1906).
- [49] W. R. D. Jones and L. Powell, *J. Inst. Met.* **67**, 177-188 (1941).
- [50] K. A. Bolshakov, N. A. Bulonkov, and M. S. Tsirlin, *Russ. J. Inorg. Chem.* **7**, 1176 (1962).
- [51] Y. K. Rao and B. V. Patil, *Metall. Trans.* **2**, 1829-1835 (1971).